PREPARATION AND CHARACTERIZATION OF WATER HYACINTH CELLULOSE/KERATOSE COMPOSITE FILMS

PATCHARIDA CHAOSRI, PRASONG SRIHANAM*

Department of Chemistry, Faculty of Science, Mahasarakham University,
Maha Sarakham 44150, Thailand

*Corresponding Author: prasong.s@msu.ac.th

Abstract:

This research aimed to extract cellulose from water hyacinth for preparation of composite films with different ratios of hair keratose. The keratose film has more transparency than other films. All films were then investigated their morphology, secondary structure, and thermal properties using scanning electron microscopy (SEM), Fourier transform infrared (FTIR) spectrophotometer, and Thermogravimetric analyzer (TGA), respectively. The results found that the native keratose film has smooth surfaces without phase separation, while the cellulose film has rough and some fibers appeared on its surface. The cellulose/keratose composite films have specific absorption peaks of each polymer functional groups. The secondary structure of the keratose film has a β-pleated sheet resulting in the fragile texture and brittle. Adding cellulose increased flexibility and thermal properties of the keratose film. This was due to the keratose and cellulose formed interaction via functional groups. The result suggested that cellulose and keratose are well compatible together. The finding results might be advantaged to use as basic information to prepare for the cellulose/keratose composite films obtaining desire properties for applications.

Keywords: Film; Cellulose; Keratose; Secondary structure; Thermal property

Introduction

The plastics from petroleum sources are gradually caused by environmental pollution. The people around the world starting to protect this problem in many ways including plastics reducing use (Pico & Barceló, 2019). Development and discovery of biodegradable polymers have been a pervasive interest to replace the plastic from petroleum sources (Liu *et al.*, 2018). Biodegradable polymers are plastics in which could be degraded by the action of living organisms in the environment, such as fungus, bacteria, or various processes in living organisms or environments. In recent year, user-friendly and eco-friendly biopolymer-based materials have been widely proposed, especially for agricultural and marine originated sources of raw materials for biopolymers (Rajabinejad *et al.*, 2018; Brodin *et al.*, 2017; Bertolino *et al.*, 2016; Sagnelli *et al.*, 2016; Kai *et al.*, 2016).

Keratose is a structural protein in which the form of keratin obtained by oxidizing extraction (Wang *et al.*, 2017; Rajabinejad *et al.*, 2018). It is water-soluble. The extracted keratoses degrade relatively fast *in vivo* and have a higher molecular weight in comparison to other types of keratin. The keratoses are highly promising candidates for encapsulation of chemicals for cosmetic, pharmaceutical and biomedical applications due to their non-toxicity, biocompatibility, biodegradability, and non-immunogenicity (Rajabinejad *et al.*, 2018).

Cellulose is one type of carbohydrate. It is a homopolymer of glucose linked together via β-1,4-glycosidic bonds (Ul-Islam *et al.*, 2012). The structure of cellulose is a mixture of hemicellulose (20-30%) and lignin (15-30%) to form the complexation structure (Lee *et al.*,

2008). Recently, the cellulose is widely applied in various industries such as food (Klemm *et al.*, 2005), pharmacy (Shokri & Adibkia, 2013), pulp and paper (Singh *et al.*, 2016), water pollution treatment (Peng *et al.*, 2019), or wine and beer (Chakraborty *et al.*, 2016). The important source of cellulose is the cell wall of the plant (Bledzki & Gassan, 1999). In this work, the cellulose was extracted from water hyacinth, a fresh plant that rapidly grown and widely spread around the world (Wissel *et al.*, 2008). The water hyacinth is a virulent cause of water pollution (Sundari & Ramesh, 2012). (Mochochoko *et al.*, 2013; Juárez-Luna *et al.*, 2019). However, it composed of a high content of cellulose (Zhu *et al.*, 2009). The goal of this work is to extract keratose from human hair and cellulose from the water hyacinth for the preparation of composite films. The films were then characterized and discussed to assess the possible way for the application of both biodegradable materials.

Materials and methods

Preparation of water hyacinth cellulose

The water hyacinth samples were collected in the Mahasarakham University then washed with tap water before cutting into small pieces. The samples were dried in an oven for 24 h and then crushed into powder. The cellulose was extracted according to previously reported (Wissel *et al.*, 2008) with some modifications. The 10 g of water hyacinth powder was digested by 100 mL 5% NaOH (w/v) with stirring and warming for 3 h. The mixture was then washed with distilled water until neutral. After dried at 90°C for 24 h, the dried sample was then bleached by 5% NaOCl (w/v) at room temperature for 24 h. The bleached samples were washed to neutral and dried at 90 °C for 24 h. Finally, the samples were hydrolyzed by 5% H_2SO_4 at 60 °C for 8 h to obtain the cellulose solution. The cellulose solution was then stirred, washed with distilled water, and filtered before use.

Preparation of keratose solution

Human hair was collected from student volunteer in Mahasarakham University, Maha Sarakham Province, Thailand. The hair was warmed to 40°C before immersing in n-hexane for 12 h to remove some lipids. Hexane, NaOH, peracetic acid, and Tris (hydroxymethyl) aminomethane used for the oxidizing extraction, and ethyl acetate used for the microparticles process, were purchased from Sigma-Aldrich®.

Keratose was obtained from human hair by using oxidizing extraction followed the method previously reported (Rajabinejad *et al.*, 2018) with some modification. The hair samples were extracted with peracetic acid with the ratio of hair: oxidizing solution of 1:30 (w/v). The mixture of hair and oxidizing reagent was left in a thermostatic water bath for 24 h at 25°C. The hair was washed to remove unreacted reagent, washed with distilled water and dried at 90°C for 1 h. The hair was then vigorously shaken in TRIS 1 M at 37°C for 2 h. The resulting solution of keratoses was filtered with a dialysis membrane (MW cut off = 3 kDa), neutralized with sodium hydroxide, and dialyzed for 3 days against distilled water. At the end of the dialysis, the solution was centrifuged to remove insoluble hair. The concentration of extracted keratose was checked by the evaporation technique and adjusted to 1.5% (w/v) with distilled water.

Preparation of cellulose/keratose composite films

The cellulose (CE) and keratose (KE) solutions with different ratios (4:0, 3:1, 1:1, 1:3, and 0:4) were prepared and stirred homogeneously for 30 min. The mixture was then cast onto a 4.5 cm diameter petri dish followed by solvent evaporation at room temperature for 24 h. The films were peeled off. The obtained films were placed in a desiccator until investigation.

Morphological observation

All of the films were dehydrated and cut into ~1cm length before observing their morphology using a scanning electron microscope (SEM) (JEOL, JSM-6460LV, Tokyo, Japan). The film fractures were coated with gold (Au) to enhance conductivity before scanning.

Secondary structure investigation

The secondary structure of films was analyzed by Fourier transform infrared (FTIR) spectroscopy (Perkin Elmer-Spectrum Gx, USA) in the spectral region of 4000-400 cm^{-1} at 4 cm^{-1} spectral resolution and 32 scans with air as reference. Before analysis, the KBr disk method was used for sample preparation.

Thermal property analysis

A thermogravimetric analyzer (TGA) (SDTQ600, TA-Instrument Co. Ltd., New Castle, DE, USA) was used for thermal stability investigation of the microparticles both with and without sample drug. Simply, 3-5 mg microparticle was heated from 50-1000°C with 20 °C/min of heating rate under nitrogen atmosphere.

Results

Transparency of films

Figure 1 shows the transparency of all films. The results indicated that the cellulose (EC) (Figure 1a) had white, dense, and lower transparency than brown keratose (KE) film (Figure 1b). The transparency and color of CE/KE composite films varied following the ratio of native polymers. All composites films have higher transparency than CE, but in lower than KE film.

Morphology of films

Figures 2 and 3 show morphology both surface (a) and cross-section (b) of films. At low magnification (Figure 2), the native CE film has a rough surface according to the random woven of fiber with clearly observed at high magnification (Figure 3). However, the CE film formed dense texture without separation as revealing by cross-section (b). The KE film has dense in texture without cracks. At high magnification, film still has a dense texture with many pores in small sizes. Considering the CE/KE composite films, the morphology of each ratio varied by the content of the polymer. At high content of cellulose (3:1), the film has a rough surface and appears fibers woven together. Increasing magnification, the texture found various

sizes of fibers at the edge of film. At the equal ratio (1:1), the composite film has a smooth surface but in lower than the KE film. Moreover, the texture of the film has a small size of particles embedded in its surface. At high content of keratose (1:3), the morphology of film was similar but smoother than the 1:1 ratio. However, the film has a crack in texture at high magnification (Figure 3).

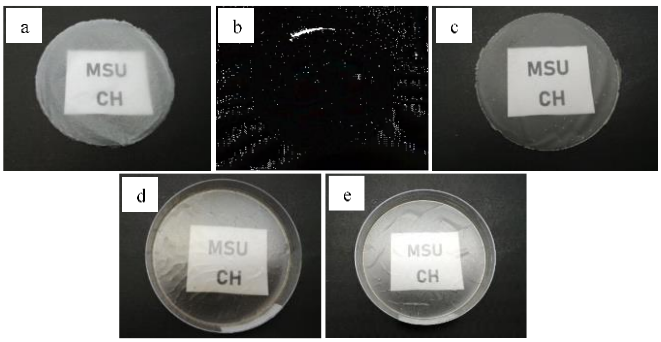

Figure 1: Transparency of films; CE (a), KE (b), CE/KE composite at 3:1 (c), 1:1 (d) and 1:3 (e) ratios.

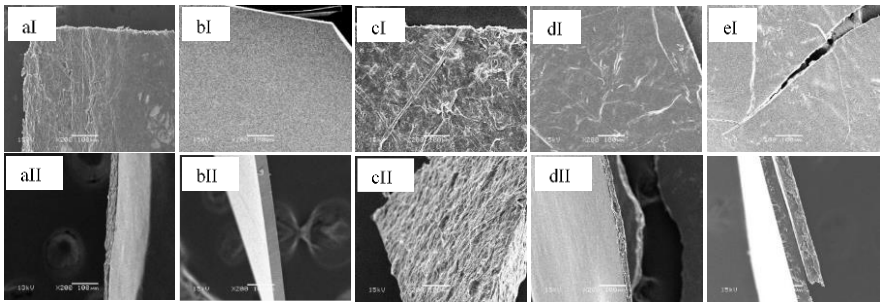

Figure 2: SEM micrographs of surface (I) and cross-section (II) of films; CE (a), KE (b), CE/KE composite at 3:1 (c), 1:1 (d) and 1:3 (e) using 200X magnification.

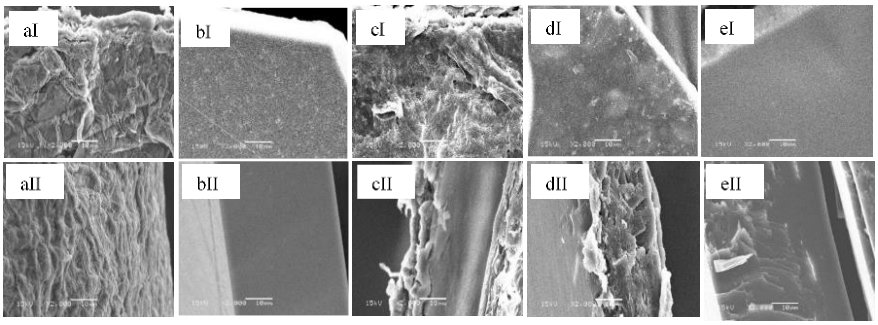

Figure 3: SEM micrographs of surface (I) and cross-section (II) of films; CE (a), KE (b), CE/KE composite at 3:1 (c), 1:1 (d) and 1:3 (e) using 2000X magnification.

Secondary structure of films

Figure 4 shows FTIR spectra of the films. The CE film indicated the absorption peaks at 3339, 2899, 1680-1519 , 1057 cm^{-1} (Figure 4a) while the absorption peaks of KE film appeared at 3205, 1678 -1519, 1042 cm^{-1} (Figure 4e). The CE/KE composite films (Figure 4b,c,d) showed variable absorption peaks depending on the content of cellulose or keratose.

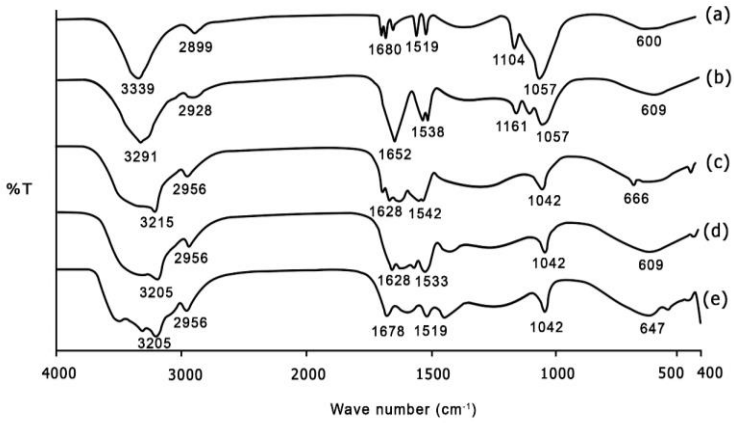

Figure 4: FTIR spectra of of films; CE (a), KE (e), CE/KE composite at 3:1 (b), 1:1 (c) and 1:3 (d).

Thermal property of films

Figure 5 shows the TG curves of films. All prepared films have decomposition peaks of more than 3 points. The first point is less than 100 °C, second is a range 150-300 °C and the third is a range of 300-400 °C. The maximum temperature of decomposition rate ($T_{d,\,max}$) of films was clearly observed by DTG curves as shown in Figure 6.

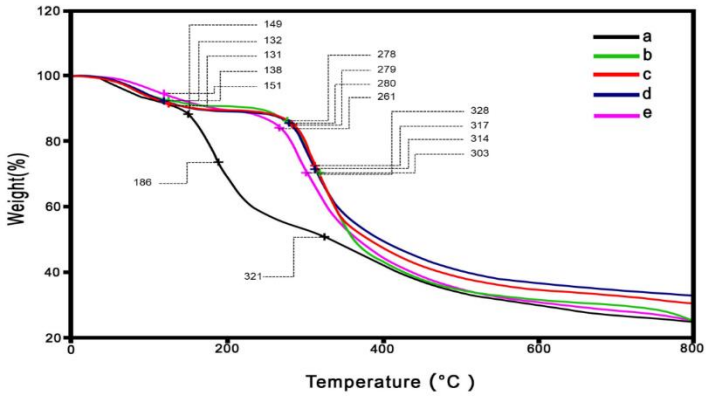

Figure 5: TG curves of films; CE (a), KE (e), CE/KE composite at 3:1 (b), 1:1 (c) and 1:3 (d).

Discussion and Conclusion

Water hyacinth is a water pollutant and caused a big problem with water pollution worldwide. It composed of the high content of cellulose which has been interested in applications. The cellulose showed good properties such as high strength, heat durability, and biodegradability. Moreover, it could be mixed with other polymers to prove some properties including poly (vinylidene fluoride) or PVDF (Zhang, 2012), silk fibroin (Zhou, 2013), and chitosan (Abdul Khalil *et al.*, 2016). SEM images indicated that the texture of cellulose film linked together without phase separation. This morphology was similar to the previous report (Qua *et al.*, 2011). However, the consistency of fiber was lower than the amino acid components in keratose. The homogeneous size of amino acids in keratose supported the transparency and smooth surfaces of the film. Considering the CE/KE composite films, the difference types and ratios used were the main factor on the film morphology.

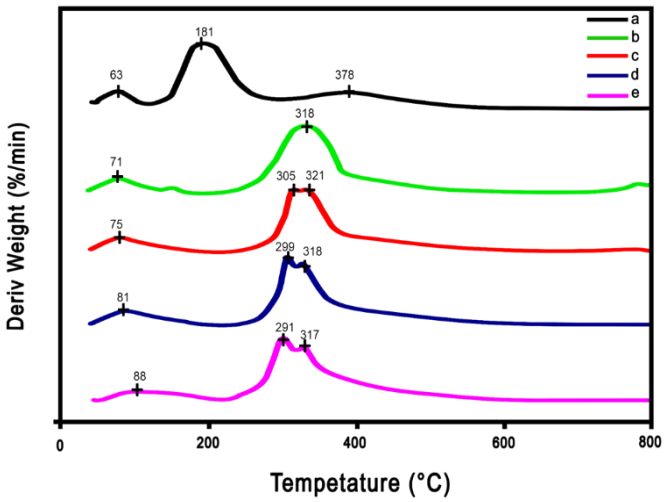

Figure 6: DTG curves of films; CE (a), KE (e), CE/KE composite at 3:1 (b), 1:1 (c) and 1:3 (d).

With FTIR spectra, cellulose film showed peaks of hydroxyl group[1] (-OH) at 3700-3000 cm^{-}, carbonyl group (C=O) at 1700-1800 cm^{-1} (Karatzos *et al.*, 2012), and the methyl group (-CH_2) at 2900-2800 cm^{-1} (Fan *et al.*, 2012). Furthermore, the peaks of hemicellulose at 1735 cm^{-1} and lignin at 1240 cm^{-1} (Sun *et al.*, 2020) were also observed. The keratose film showed absorption peaks of the amide group (R-COONH-R), which the main bonding of amino acids. Amide I (1700-1600 cm^{-1}) is the responsible peak of the carbonyl group (-CO-), amide II (1600-1500 cm^{-1}) is responsible peak of amine group (-NH-) and methyl group (-CH-), and amide III (1300-1150 cm^{-1}) is a responsible peak of -CN- stretching, plane -NH-, -C-C- and -CO- stretching (Sharma *et al.*, 2017). The absorption peak at 1040 cm^{-1} confirmed cysteic acid group of the oxidized keratin (keratose) (Pakkaner *et al.*, 2019). The absorption peaks from FTIR spectra indicated that the keratose film has a β-sheet structure. This film has rapidly brittle and very hard to manual. The high content of hydroxyl groups in cellulose supported the hydrophilic property of the film. This helped to increase the flexibility of the film. The mixture of cellulose and keratose resulted to change of the absorption peaks of the main functional

groups. However, they still appeared in all of the main groups which varied by the ratio of the polymer. The keratose supported the strength of cellulose film while cellulose helped to decrease the brittle of keratose. This suggested that cellulose and keratose were good compatibilities via interaction formation such as hydrogen bonds, hydrophobic interaction, and van der valve force. Films showed decomposition peaks at least 3 points. At lower 100 °C is caused by water evaporation in polymer molecules (Dou *et al.*, 2019). The temperatures in the range of 150-300 °C are the decomposition point of hemicellulose and lignin and 300-400 °C are the decomposition of cellulose chain. The keratose showed a decomposition point in the range of 250-300 °C (Rajabinejad *et al.*, 2018). The composite films showed variable decomposition points depending on the ratio used as like as the thermal property. Cellulose content helped to increase the thermal property of the films. However, the highest $T_{d, max}$ found in the composite film at 1:1 ratio. This result confirmed the compatibility of the cellulose and keratose.

In conclusion, the properties of films depended on many factors such as type of polymer, the mixed ratio as well as the preparation methods. The results obtained from this work suggested that the cellulose could be extracted from the wastewater hyacinth. This cellulose could also be used as a biodegradable polymer for blending with keratose or other materials for value-added and replaced of non-degradable polymer like synthetic plastics.

Acknowledgement

This research was financially supported by Faculty of Science, Mahasarakham University (Grant year 2020).

References

Abdul Khalil, H.P.S, Saurabh, C.K., Adnan, A.S., Nurul Fazita, M.R., Syakir, M.I., Davoudpour, Y., Rafatullah, M. Abdullah, C.K., Haafiz, M.K.M. & Dungani, R. (2016). A review on chitosan-cellulose blends and nanocellulose reinforced chitosan biocomposites: Properties and their applications. *Carbohydrate Polymers*, 150, 216-226.

Bertolino, V., Cavallaro, G., Lazzara, G., Merli, M., Milioto, S., Parisi, F. & Sciascia, L. (2016). Effect of the biopolymer charge and the nanoclay morphology on nanocomposite materials. *Industrial & Engineering Chemistry Research*, 55, 7373-7380.

Bledzki, A.K. & Gassan, J. (1999). Composites reinforced with cellulose based fibres. *Progress in Polymer Science*, 24, 221-274.

Brodin, M., Vallejos, M., Opedal, M.T., Area, M.C. & Chinga-Carrasco, G. (2017). Lignocellulosics as sustainable resources for production of bioplastics - a review. *J. Clean. Prod*. 162, 646-664.

Chakraborty, S., Gupta, R., Jain, K.K., Hemansi, Gautam, S. & Kuhad, R.C. (2016). Cellulases: Application in wine and brewery industry. New and Future Developments in Microbial Biotechnology and Bioengineering, pp. 193-200.

Dou, J., Bian, H., Yelle, D.J., Ago, M., Vajanto, K., Vuorinen, T. & Zhu, J. (2019). Lignin containing cellulose nanofibril production from willow bark at 80 °C using a highly recyclable acid hydrotrope. *Industrial Crops and Products*, 129, 15-23.

Fan, M., Dai, D. & Huang, B. (2012). Fourier transform infrared spectroscopy for natural fibres. Fourier Transform - Materials Analysis, In Tech, Shanghai, pp. 45-68.

Juárez-Lunaa, G.N., Favela-Torresa, E., Quevedob, I.R. & Batina, N. (2019). Enzymatically assisted isolation of high-quality cellulose nanoparticles from water hyacinth stems. *Carbohydrate Polymers*, 220, 110-117.

Kai, D., Tan, M.J., Chee, P.L., Chua, Y.K., Yap, Y.L. & Loh X.J. (2016). Towards lignin-based functional materials in a sustainable world. *Green Chemistry*, 18, 1175-1200.

Karatzos, S.K., Edye, L.A., Orlando, W. & Doherty, S. (2012). Sugarcane bagasse pretreatment using three imidazolium-based ionic liquids; mass balances and enzyme kinetics. *Biotechnology for Biofuels*, 5, 1-12.

Klemm, D., Heublein, B., Fink, H.P. & Bohn, A. (2005). Cellulose: fascinating biopolymer and sustainable raw material. *Angewandte Chemie International Edition*, 44, 3358-3393.

Lee, J.S., Parameswaran, B., Lee, J.P. & Park, S.C. (2008). Recent Developments of Key Technologies on Cellulosic Ethanol Production. *Journal of Scientific & Industrial Research*, 67, 865-873.

Liu, R., Dai, L., Zou, Z. & Si, C. (2018). Drug-loaded poly (L-lactide)/lignin stereocomplex film for enhancing stability and sustained release of trans-resveratrol. *International Journal of Biological Macromolecule*, 119, 1129-1136.

Mochochoko, T., Oluwafemi, O.S., Jumbam, D.N. & Songca. S.P. (2013). Green synthesis of silver nanoparticles using cellulose extracted from an aquatic weed; water hyacinth. *Carbohydrate Polymers*, 98, 290-294.

Pakkaner, E., Yalçın, D., Uysal, B. & Top, A. (2019). Self-assembly behavior of the keratose proteins extracted from oxidized Ovis aries wool fibers. *International Journal of Biological Macromolecules*, 125, 1008-1015.

Peng, B., Yao, Z., Wang, X., Crombeen, M., Gsweene, D. & Tam, K.C. (2019). Cellulose-based materials in wastewater treatment of petroleum industry. *Green Energy & Environment*, 5, 37-49.

Picó, Y. & Barceló, D. (2019). Analysis and prevention of microplastics pollution in water: current perspectives and future directions. *ACS*, 4, 6709-6719.

Qua, E.H., Hornsby, P.R., Sharma, H.S.S. & Lyons, G. (2011). Preparation and characterisation of cellulose nanofibres. *Journal of Materials Science*, 46, 6029-6045.

Rajabinejad, H., Patrucco, A., Caringella, R., Montarsolo, A., Zoccola, M. & Davide Pozzo, P. (2018). Preparation of keratin-based microcapsules for encapsulation of hydrophilic molecules. *Ultrasonics Sonochemistry*, 40, 527-532.

Rajabinejad, H., Patrucco, A., Montarsolo, A., Rovero, G. & Tonin, C. (2018). Physicochemical properties of keratin extracted from wool by various methods. *Textile Research Journal*, 88, 2018.

Sagnelli, D., Hebelstrup, K.H., Leroy, E., Rolland-Sabaté, A., Guilois, S., Kirkensgaard, J.J.K., Mortensen, K., Lourdin, D. & Blennow A. (2016). Plant-crafted starches for bioplastics production. *Carbohydrate Polymers*. 152, 398-408.

Sharma, S., Gupta, A., Chik, S.M.S.T., Kee, C.G., Mistry, B.M., Kim, D.H. & Sharma, G. (2017). Characterization of keratin microparticles from feather biomass with potent antioxidant and anticancer activities. *International Journal of Biological Macromolecules*, 104, 189-196.

Shokri, J. & Adibkia, K. (2013). Application of cellulose and cellulose derivatives in pharmaceutical industries. Cellulose - medical, pharmaceutical and electronic applications, In Tech, pp. 47.

Singh, S., Singh, V.K., Aamir, M., Dubey, M.K., Patel, J.S., Upadhyay, R.S. & Gupta, V.K. (2016). Cellulase in Pulp and Paper Industry. New and Future Developments in Microbial Biotechnology and Bioengineering, pp. 152-162.

Sundari, M.T. & Ramesh, A. (2012). Isolation and characterization of cellulose nanofibers from the aquatic weed water hyacinth-*Eichhornia crassipes*. *Carbohydrate Polymers*, 87, 1701-1705.

Sun, D., Onyianta, A.J., O'Rourke, D., Perrin, G., Popescu, C.-M., Saw, L.H., Cai, Z. & Dorris, M. (2020). A process for deriving high quality cellulose nanofibrils from water hyacinth invasive species. *Cellulose*, 27, 3727-3740.

Ul-Islam, M., T. Khan, & J.K. Park. (2012). Water holding and release properties of bacterial cellulose obtained by in situ and ex situ modification. *Carbohydrate Polymers*. 88(2), 596-603.

Wang, J., Hao, S., Luo, T., Zhou, T., Yang, X. & Wang, B. (2017). Keratose/poly (vinyl alcohol) blended nanofibers: Fabrication and biocompatibility assessment. *Mater. Sci. Eng*. C 72, 212-219.

Wissel, H., Mayr, C. & Lücke, A. (2008). A new approach for the isolation of cellulose from aquatic plant tissue and freshwater sediments for stable isotope analysis. *Organic Geochemistry*, 39, 1545-1561.

Zhang, X., Feng, J., Liu, X. & Zhu, J. (2012). Preparation and characterization of regenerated cellulose/poly (vinylidene fluoride) (PVDF) blend films. *Carbohydrate Polymers*, 89(1), 67-71.

Zhou, L., Wang, Q., Wen, J., Chen, X. & Shao, Z. (2013). Preparation and characterization of transparent silk fibroin/cellulose blend films. *Polymer*, 54(18), 5035-5042.

Zhu, Y.L., Zayed A.M., Qian, J.H., de Souza, M. & Terry, N. (1999). Phytoaccumulation of trace elements by wetland plants: II. Water hyacinth. *Journal of Environmental Quality*, 28, 339e344.